A comprehensive study on the semileptonic decay of heavy flavor mesons

Zhang Lu

College of Nuclear Science and Technology, Beijing Normal University

2021 年 3 月 27 日

Xian-Wei Kang, Xin-Heng Guo

JHEP 02(2021)179, [arXiv:2012.04417]

第二届强子与重味物理理论与实验联合研讨会　兰州　兰州大学

Motivation

- Extraction of CKM matrix elements

  The deviation from the unitarity relation encoded in the CKM matrix

  $\longrightarrow$ an inspiring signal of New Physics

  The semileptonic decay offers a clean environment

- The lepton-flavor universality violation

- More physical observables

  distinguish various model predictions

Contents

- Form factors and Helicity amplitudes
- Differential decay distribution
- The physical observables
- Results
- Summary

- D, D_s, B and B_s

The semileptonic decay of D meson to a pseudoscalar (P) or a vector (V) meson.

$$\begin{aligned} \mathcal{M}\left(D \rightarrow P(V) l^{+} \nu_l\right) &= \frac{G_F}{\sqrt{2}} V_{cq} \left\langle P(V) \mid \bar{q} O^{\mu} c \mid D_{(s)} \right\rangle l^{+} O_{\mu} \nu_l \\ &= \frac{G_F}{\sqrt{2}} V_{cq} H^{\mu} L_{\mu}, \end{aligned} \tag{1}$$

- The invariant matrix element:

$$\langle P(p_2)|V_\mu|D(p_1)\rangle = T_\mu, \quad \langle V(p_2)|V_\mu - A_\mu|D(p_1)\rangle = \epsilon_2^{\dagger\nu} T_{\mu\nu}. \tag{2}$$

- The form factors, Bauer-Stech-Wirbel (BSW) form

$$\begin{aligned} T_\mu &= \left(P_\mu - \frac{m_1^2 - m_2^2}{q^2} q_\mu\right) F_1(q^2) + \frac{m_1^2 - m_2^2}{q^2} q_\mu F_0(q^2), \\ T_{\mu\nu} &= -(m_1 + m_2)\left[g_{\mu\nu} - \frac{P_\nu}{q^2} q_\mu\right] A_1(q^2) + \frac{P_\nu}{m_1 + m_2}\left[P_\mu - \frac{m_1^2 - m_2^2}{q^2} q_\mu\right] A_2(q^2) \\ &\quad - 2m_2 \frac{P_\nu}{q^2} q_\mu A_0(q^2) + \frac{i}{m_1 + m_2} \varepsilon_{\mu\nu\alpha\beta} P^\alpha q^\beta V(q^2). \end{aligned} \tag{3}$$

where $P_\mu = (p_1 + p_2)_\mu$, $q_\mu = (p_1 - p_2)_\mu$.

Form factors and Helicity amplitudes

Four-vectors $\epsilon^{\mu}(\lambda_W)$:

orthonormality property $\epsilon^{\dagger}_{\mu}(\lambda_W)\epsilon^{\mu}(\lambda'_W) = g_{\lambda_W \lambda'_W}$;

completeness relations: $\epsilon_{\mu}(\lambda_W)\epsilon^{\dagger}_{\nu}(\lambda'_W)g_{\lambda_W \lambda'_W} = g_{\mu\nu}$.

- The contraction of leptonic and hadronic tensors:

$$\begin{aligned} L^{\mu\nu} H_{\mu\nu} &= L_{\mu'\nu'} g^{\mu'\mu} g^{\nu'\nu} H_{\mu\nu} \\ &= L\left(\lambda_W, \lambda'_W\right) g_{\lambda_W \lambda''_W} g_{\lambda'_W \lambda'''_W} H\left(\lambda''_W \lambda'''_W\right). \end{aligned} \tag{4}$$

- In the helicity-component space:

$$L\left(\lambda_W, \lambda'_W\right) = \epsilon^{\mu}(\lambda_W)\epsilon^{\dagger\nu}(\lambda'_W)L_{\mu\nu}, \quad H\left(\lambda_W, \lambda'_W\right) = \epsilon^{\dagger\mu}(\lambda_W)\epsilon^{\nu}(\lambda'_W)H_{\mu\nu}. \tag{5}$$

- For the transition $D \to Pl^+\nu_l$, the helicity amplitudes:

$$H_{\lambda_W} \equiv \epsilon^{\mu\dagger}(\lambda_W) T_\mu \tag{6}$$

The relations between form factors and helicity amplitudes:

$$H_t = \frac{1}{\sqrt{q^2}}(m_1^2 - m_2^2)F_0(q^2),$$
$$H_\pm = 0,$$
$$H_0 = \frac{2m_1|\vec{p}_2|}{\sqrt{q^2}}F_1(q^2).$$

Form factors and Helicity amplitudes

- For the transition $D \to V l^+ \nu_l$, the helicity amplitudes:

$$H_{\lambda_W \lambda_V} \equiv \epsilon^{\dagger\mu}(\lambda_W)\epsilon_2^{\dagger\alpha}(\lambda_V) T_{\mu\alpha} \qquad (7)$$

The relations:

$$H_t \equiv \epsilon^{\dagger\mu}(t)\epsilon_2^{\dagger\nu}(0)T_{\mu\nu} = -\frac{2m_1|\vec{p}_2|}{\sqrt{q^2}}A_0(q^2),$$

$$H_\pm \equiv \epsilon^{\dagger\mu}(\pm)\epsilon_2^{\dagger\nu}(\pm)T_{\mu\nu} = -(m_1+m_2)A_1(q^2) \pm \frac{2m_1|\vec{p}_2|}{m_1+m_2}V(q^2),$$

$$H_0 \equiv \epsilon^{\dagger\mu}(0)\epsilon_2^{\dagger\nu}(0)T_{\mu\nu} = -\frac{m_1+m_2}{2m_2\sqrt{q^2}}\left(m_1^2-m_2^2-q^2\right)A_1(q^2) + \frac{1}{m_1+m_2}\frac{2m_1^2|\vec{p}_2|^2}{m_2\sqrt{q^2}}A_2(q^2).$$

The differential decay distribution

In the three-body phase, $\sum_{\text{spins}} |\mathcal{M}|^2 = \frac{G_F^2}{2} |V_{cq}|^2 L\left(\lambda_W, \lambda'_W\right) g_{\lambda_W \lambda''_W} g_{\lambda'_W \lambda'''_W} H\left(\lambda''_W, \lambda'''_W\right)$

- Hadronic part $H\left(\lambda_W, \lambda'_W\right) = \begin{cases} H_{\lambda_W} H^{\dagger}_{\lambda'_W}, & D \to P, \\ H_{\lambda_W \lambda_V} H^{\dagger}_{\lambda'_W \lambda_V}, & D \to V. \end{cases}$

- Leptonic part

$$L_{\mu\nu} = \begin{cases} \mathrm{tr}\left[\left(\not{k}_1 + m_l\right) O_\mu \not{k}_2 O_\nu\right], & W^- \to l^- \bar{\nu}_l, \\ \mathrm{tr}\left[\left(\not{k}_1 - m_l\right) O_\nu \not{k}_2 O_\mu\right], & W^+ \to l^+ \nu_l, \end{cases}$$

$$= 8\left(k_{1\mu} k_{2\nu} + k_{1\nu} k_{2\mu} - k_1 \cdot k_2 g_{\mu\nu} \pm i\varepsilon_{\mu\nu\alpha\beta} k_1^\alpha k_2^\beta\right)$$

The differential decay distribution

- Two-fold differential decay distribution:

$$\frac{d\Gamma\left(D\to P(V)l^{+}\nu_l\right)}{dq^2 d\cos\theta}=\frac{G_F^2|V_{cq}|^2|\vec{p}_2|q^2v^2}{32(2\pi)^3m_1^2}\times\left[\left(1+\cos^2\theta\right)\mathcal{H}_U+2\sin^2\theta\mathcal{H}_L+2\cos\theta\mathcal{H}_P\right.$$
$$\left.+2\delta_l\left(\sin^2\theta\mathcal{H}_U+2\cos^2\theta\mathcal{H}_L+2\mathcal{H}_S-4\cos\theta\mathcal{H}_{SL}\right)\right].\tag{8}$$

- The differential q^2 distribution:

$$\frac{d\Gamma\left(D\to P(V)l^{+}\nu_l\right)}{dq^2}=\frac{G_F^2|V_{cq}|^2|\vec{p}_2|q^2v^2}{12(2\pi)^3m_1^2}\times\left[\mathcal{H}_U+\mathcal{H}_L+\delta_l\left(\mathcal{H}_U+\mathcal{H}_L+3\mathcal{H}_S\right)\right]\tag{9}$$

The differential decay distribution

- Definitions of helicity structure functions

Parity-conserving	Parity-violating
$\mathcal{H}_U = \|H_+\|^2 + \|H_-\|^2$	$\mathcal{H}_P = \|H_+\|^2 - \|H_-\|^2$
$\mathcal{H}_L = \|H_0\|^2$	$\mathcal{H}_A = \frac{1}{2}\mathrm{Re}(H_+H_0^\dagger - H_-H_0^\dagger)$
$\mathcal{H}_T = \mathrm{Re}(H_+H_-^\dagger)$	$\mathcal{H}_{IA} = \frac{1}{2}\mathrm{Im}(H_+H_0^\dagger - H_-H_0^\dagger)$
$\mathcal{H}_{IT} = \mathrm{Im}(H_+H_-^\dagger)$	$\mathcal{H}_{SA} = \frac{1}{2}\mathrm{Re}(H_+H_t^\dagger - H_-H_t^\dagger)$
$\mathcal{H}_I = \frac{1}{2}\mathrm{Re}(H_+H_0^\dagger + H_-H_0^\dagger)$	$\mathcal{H}_{ISA} = \frac{1}{2}\mathrm{Im}(H_+H_t^\dagger - H_-H_t^\dagger)$
$\mathcal{H}_{II} = \frac{1}{2}\mathrm{Im}(H_+H_0^\dagger + H_-H_0^\dagger)$	
$\mathcal{H}_S = \|H_t\|^2$	
$\mathcal{H}_{ST} = \frac{1}{2}\mathrm{Re}(H_+H_t^\dagger + H_-H_t^\dagger)$	
$\mathcal{H}_{IST} = \frac{1}{2}\mathrm{Im}(H_+H_t^\dagger + H_-H_t^\dagger)$	
$\mathcal{H}_{SL} = \mathrm{Re}(H_0H_t^\dagger)$	
$\mathcal{H}_{ISL} = \mathrm{Im}(H_0H_t^\dagger)$	
$\mathcal{H}_{tot} = \mathcal{H}_U + \mathcal{H}_L + \delta_l\,(\mathcal{H}_U + \mathcal{H}_L + 3\mathcal{H}_S)$	

The differential decay distribution

The cascade decay $D \to V(\to P_1 P_2) l \nu_l$

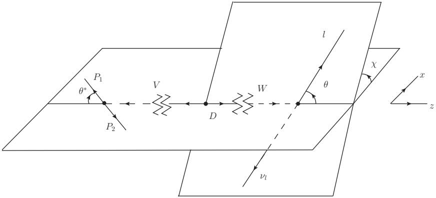

- amplitude $\mathcal{A}(V \to P_1 P_2) = g_{VPP} \cdot \epsilon_2^{\rho}(\lambda_V) \cdot p_{3\rho}$

The hadronic tensor:

$$\begin{aligned} H\left(\lambda_W, \lambda'_W\right) &= \epsilon^{\dagger\mu}(\lambda_W)\epsilon^{\nu}(\lambda'_W) H_{\mu\nu} \\ &= g_{VPP}^2 p_{3\alpha'} p_{3\beta'} \epsilon_2^{\alpha'}(\lambda_V)\epsilon_2^{\dagger\beta'}(\lambda'_V) \times H_{\lambda_W,\lambda_V} H^{\dagger}_{\lambda'_W,\lambda'_V}. \end{aligned} \tag{10}$$

- The fourfold distribution for the cascade:

$$\frac{d\Gamma\left(D \to V(\to P_1 P_2) l^+ \nu_l\right)}{dq^2 d\cos\theta d\frac{\chi}{2\pi} d\cos\theta^*} = \frac{G_F^2 |V_{cq}|^2 |\vec{p}_2| q^2 v^2}{12(2\pi)^3 m_1^2} Br(V \to P_1 P_2) W(\theta, \theta^*, \chi), \tag{11}$$

The differential decay distribution

- the angular distribution $W(\theta, \theta^*, \chi)$:

$$
\begin{aligned}
W(\theta, \theta^*, \chi) =& \frac{9}{32}\left(1+\cos^2\theta\right)\sin^2\theta^*\mathcal{H}_U + \frac{9}{8}\sin^2\theta\cos^2\theta^*\mathcal{H}_L + \frac{9}{16}\cos\theta\sin^2\theta^*\mathcal{H}_P \\
& - \frac{9}{16}\sin^2\theta\sin^2\theta^*\cos 2\chi\mathcal{H}_T + \frac{9}{8}\sin\theta\sin 2\theta^*\cos\chi\mathcal{H}_A \\
& + \frac{9}{16}\sin 2\theta\sin 2\theta^*\cos\chi\mathcal{H}_I - \frac{9}{8}\sin\theta\sin 2\theta^*\sin\chi\mathcal{H}_{II} \\
& - \frac{9}{16}\sin 2\theta\sin 2\theta^*\sin\chi\mathcal{H}_{IA} + \frac{9}{16}\sin^2\theta\sin^2\theta^*\sin 2\chi\mathcal{H}_{IT} \\
& + \delta_l\left[\frac{9}{4}\cos^2\theta^*\mathcal{H}_S - \frac{9}{2}\cos\theta\cos^2\theta^*\mathcal{H}_{SL} + \frac{9}{4}\cos^2\theta\cos^2\theta^*\mathcal{H}_L\right. \\
& + \frac{9}{16}\sin^2\theta\sin^2\theta^*\mathcal{H}_U + \frac{9}{8}\sin^2\theta\sin^2\theta^*\cos 2\chi\mathcal{H}_T \\
& + \frac{9}{4}\sin\theta\sin 2\theta^*\cos\chi\mathcal{H}_{ST} - \frac{9}{8}\sin 2\theta\sin 2\theta^*\cos\chi\mathcal{H}_I \\
& - \frac{9}{4}\sin\theta\sin 2\theta^*\sin\chi\mathcal{H}_{ISA} + \frac{9}{8}\sin 2\theta\sin 2\theta^*\sin\chi\mathcal{H}_{IA} \\
& \left. - \frac{9}{8}\sin^2\theta\sin^2\theta^*\sin 2\chi\mathcal{H}_{IT}\right].
\end{aligned}
$$

More physical observables

To study the effect of the lepton mass and provide a more detailed physical picture in semileptonic decays beyond the branching fraction, we can also define other physical observables that can be measured experimentally.

- The forward-backward asymmetry:

$$\mathcal{A}_{FB}^{l}(q^2) = \frac{\int_0^1 d\cos\theta \frac{d\Gamma}{dq^2 d\cos\theta} - \int_{-1}^{0} d\cos\theta \frac{d\Gamma}{dq^2 d\cos\theta}}{\int_0^1 d\cos\theta \frac{d\Gamma}{dq^2 d\cos\theta} + \int_{-1}^{0} d\cos\theta \frac{d\Gamma}{dq^2 d\cos\theta}} = \frac{3}{4}\frac{H_P - 4\delta_l H_{SL}}{H_{tot}}. \quad (12)$$

More physical observables

The leptonic polarization

set the azimuthal angel $\chi = 0$, spin four-vector $s^\mu = \left(\frac{\vec{k}_1 \cdot \hat{\vec{s}}}{m_l}, \ \hat{\vec{s}} + \frac{\vec{k}_1 (\vec{k}_1 \cdot \hat{\vec{s}})}{m_l (k_1^0 + m_l)} \right)$

- The longitudinal polarization vector $s_L^\mu = \frac{1}{m_l} \left(|\vec{k}_1|, \ E_1 \sin\theta, \ 0, \ E_1 \cos\theta \right)$
- The corresponding leptonic tensor:

$$L_{\mu\nu}(s_L) = \mp 8 m_l \left(s_{L\mu} k_{2\nu} + s_{L\nu} k_{2\mu} - s_L \cdot k_2 g_{\mu\nu} \pm i \varepsilon_{\mu\nu\alpha\beta} s_L^\alpha k_2^\beta \right) \tag{13}$$

More physical observables

- The polarized differential decay distribution:

$$\frac{d\Gamma(s_L)}{dq^2} = \frac{G_F^2 |V_{cq}|^2 |\vec{p}_2| q^2 v^2}{12(2\pi)^3 m_1^2} \left[\mathcal{H}_U + \mathcal{H}_L - \delta_l \left(\mathcal{H}_U + \mathcal{H}_L + 3\mathcal{H}_S\right)\right]. \tag{14}$$

- The longitudinal polarization of lepton:

$$P_L^l(q^2) = \frac{d\Gamma(s_L)}{dq^2} \Big/ \frac{d\Gamma}{dq^2} = \frac{\mathcal{H}_U + \mathcal{H}_L - \delta_l \left(\mathcal{H}_U + \mathcal{H}_L + 3\mathcal{H}_S\right)}{\mathcal{H}_{tot}} \tag{15}$$

- The transverse polarization corresponding to the vector $s_T^\mu = \left(0,\ \hat{\vec{s}}_T\right) = (0,\ \cos\theta,\ 0,\ -\sin\theta)$:

$$P_T^l(q^2) = -\frac{3\pi\sqrt{\delta_l}}{4\sqrt{2}} \frac{\mathcal{H}_P + 2\mathcal{H}_{SL}}{\mathcal{H}_{tot}}. \tag{16}$$

More physical observables

- Normalized angle distribution $\widetilde{W}(\theta^*, \theta, \chi) = \frac{W(\theta^*,\theta,\chi)}{\mathcal{H}_{tot}}$
- the normalized θ and θ^* angular distribution:

$$\begin{aligned} \widetilde{W}(\theta) &= \frac{W(\theta)}{\mathcal{H}_{tot}} = \frac{a + b\cos\theta + c\cos^2\theta}{2\,(a + c/3)} \\ \widetilde{W}(\theta^*) &= \frac{W(\theta^*)}{\mathcal{H}_{tot}} = \frac{a' + c'\cos^2\theta^*}{2a' + 2/3c'} \end{aligned} \tag{17}$$

- the leptonic convexity parameter $C_F^l(q^2) = \frac{d^2\widetilde{W}(\theta)}{d(\cos\theta)^2}$
- The hadronic convexity parameter $C_F^h(q^2) = \frac{d^2\widetilde{W}(\theta^*)}{d(\cos\theta^*)^2}$

More physical observables

- The longitudinal polarization fraction of the final vector meson:

$$F_L^l(q^2) = \frac{d\Gamma(\lambda_V = 0)/dq^2}{d\Gamma/dq^2} = \frac{(1+\delta_l)\mathcal{H}_L + 3\delta_l\mathcal{H}_S}{\mathcal{H}_{tot}} \tag{18}$$

- The transverse polarization fraction is $F_T^l(q^2) = 1 - F_L^l(q^2)$

- the trigonometric moments:

$$W_i = \int d\cos\theta d\cos\theta^* d(\chi/2\pi) M_i(\theta,\theta^*,\chi) \widetilde{W}(\theta,\theta^*,\chi) = \langle M_i(\theta,\theta^*,\chi)\rangle\,. \tag{19}$$

$$\begin{aligned} W_T(q^2) &= \langle\cos 2\chi\rangle = -\frac{1}{2}(1-2\delta_l)\frac{\mathcal{H}_T}{\mathcal{H}_{tot}}, \\ W_I(q^2) &= \langle\cos\theta\cos\theta^*\cos\chi\rangle = \frac{9\pi^2(1-2\delta_l)}{512}\frac{\mathcal{H}_I}{\mathcal{H}_{tot}}, \\ W_A(q^2) &= \langle\sin\theta\sin\theta^*\cos\chi\rangle = \frac{3\pi}{16}\frac{\mathcal{H}_A + 2\delta_l\mathcal{H}_{ST}}{\mathcal{H}_{tot}}. \end{aligned} \tag{20}$$

Average value

- Average value, reinstate the phase factor $C(q^2) = |\vec{p}_2|\,(q^2 - m_l^2)^2/q^2$:

$$\langle \mathcal{A}_{FB}^{l} \rangle = \frac{3}{4} \frac{\int dq^2\, C(q^2)\, (\mathcal{H}_P - 4\delta_l \mathcal{H}_{SL})}{\int dq^2\, C(q^2)\, [\mathcal{H}_U + \mathcal{H}_L + \delta_l\, (\mathcal{H}_U + \mathcal{H}_L + 3\mathcal{H}_S)]}. \quad (21)$$

A similar operation holds for all others.

The results

For the related form factors in these physical quantities equations, we stick to the predictions in the covariant light-front quark model (CLFQM).

H.-Y.Cheng, C.-K.Chua, and C.-W.Hwang, Phys.Rev.D 69,074025(2004)

R. Verma, J.Phys.G 39,025005(2012)

- The momentum dependence of form factors can be parameterized as:

$$F(q^2) = \frac{F(0)}{1 - a\left(q^2/m_D^2\right) + b\left(q^2/m_D^2\right)^2} \tag{22}$$

- For the final state of the $D_{(s)}$ transitions, the pseudoscalar mesons P contain η, η', π^0, K^0, $\bar{K}^0$ and the vector mesons V contain $\rho, \omega, \phi, K^*, \bar{K}^*$;
- For the $B_{(s)}$ transitions, the pseudoscalar mesons P contain $\eta, \eta', \pi^0, \bar{D}^0, D_s^-$ and the vector mesons V contain $\rho, \omega, K^{*-}, \bar{D}^{*0}, D_s^{*-}$.

The results

- Branching fraction, compared to the PDG and BESIII results. All values are in unit of 10^{-3}

		e mode			μ mode		
		CLFQM	PDG	BESIII	CLFQM	PDG	BESIII
$D^+ \to P$	$D^+ \to \eta l^+ \nu_l$	1.20	1.11 ± 0.07		1.16		1.04 ± 0.15 [47]
	$D^+ \to \eta' l^+ \nu_l$	0.179	0.20 ± 0.04		0.169		
	$D^+ \to \pi^0 l^+ \nu_l$	4.09	3.72 ± 0.17	3.63 ± 0.13 [48]	4.04	3.50 ± 0.15	
	$D^+ \to \bar{K}^0 l^+ \nu_l$	103.2	87.3 ± 1.0	86.0 ± 2.1 [48]	100.7	87.6 ± 1.9	
$D^+ \to V$	$D^+ \to \rho l^+ \nu_l$	2.32	$2.18^{+0.17}_{-0.25}$		2.22	2.4 ± 0.4	
	$D^+ \to \omega l^+ \nu_l$	2.07	1.69 ± 0.11	1.69 ± 0.11 [49]	1.98		1.77 ± 0.29 [49]
	$D^+ \to \bar{K}^{*0} l^+ \nu_l$	73.2	54.0 ± 1.0		69.3	52.7 ± 1.5	
$D_s^+ \to P$	$D_s^+ \to \eta l^+ \nu_l$	21.9	23.2 ± 0.8	23.0 ± 3.9 [50]	21.5	24 ± 5.0	24.2 ± 5.7 [50]
	$D_s^+ \to \eta' l^+ \nu_l$	8.82	8.0 ± 0.7	9.3 ± 3.5 [50]	8.41	11 ± 5.0	10.6 ± 6.1 [50]
	$D_s^+ \to K^0 l^+ \nu_l$	2.54	3.4 ± 0.4		2.49		
$D_s^+ \to V$	$D_s^+ \to \phi l^+ \nu_l$	30.7	23.9 ± 1.6	22.6 ± 5.4 [50]	28.9	19.0 ± 5.0	19.4 ± 6.2 [50]
	$D_s^+ \to K^{*0} l^+ \nu_l$	1.90	2.15 ± 0.28		1.82		

- Cross checked: be calculated directly via form factors
  H.-Y.Cheng and X.-W.Kang, Eur.Phys.J.C77,587(2017)
- The experimental data:
  PDG: Phys. Rev. D 98, 030001 (2018)
  BESIII: Phys.Rev.Lett. 124,231801(2020), Phys.Rev.D 96,012002(2017), Phys.Rev.D 101,072005(2020)

The results

- Branching fraction for the semileptonic decays of B^+ and B_s, compared to the PDG results.

		e mode	PDG ($l^+\nu_l$)	τ mode	PDG ($\tau^+\nu_\tau$)
$B^+ \to P$	$B^+ \to \eta l^+\nu_l$	4.96×10^{-5}	$(3.9 \pm 0.5) \times 10^{-5}$	3.03×10^{-5}	
	$B^+ \to \eta' l^+\nu_l$	2.41×10^{-5}	$(2.3 \pm 0.8) \times 10^{-5}$	1.28×10^{-5}	
	$B^+ \to \pi^0 l^+\nu_l$	7.20×10^{-5}	$(7.8 \pm 0.27) \times 10^{-5}$	4.89×10^{-5}	
	$B^+ \to \bar{D}^0 l^+\nu_l$	2.59×10^{-2}	$(2.35 \pm 0.09) \times 10^{-2}$	0.78×10^{-2}	$(0.77 \pm 0.25) \times 10^{-2}$
$B^+ \to V$	$B^+ \to \rho l^+\nu_l$	2.00×10^{-4}	$(1.58 \pm 0.11) \times 10^{-4}$	1.09×10^{-4}	
	$B^+ \to \omega l^+\nu_l$	1.89×10^{-4}	$(1.19 \pm 0.09) \times 10^{-4}$	1.00×10^{-4}	
	$B^+ \to \bar{D}^{*0} l^+\nu_l$	6.67×10^{-2}	$(5.66 \pm 0.22) \times 10^{-2}$	1.66×10^{-2}	$(1.88 \pm 0.20) \times 10^{-2}$
$B_s \to P$	$B_s \to K^- l^+\nu_l$	9.23×10^{-5}		6.18×10^{-5}	
	$B_s \to D_s^- l^+\nu_l$	2.41×10^{-2}		0.72×10^{-2}	
$B_s \to V$	$B_s \to K^{*-} l^+\nu_l$	3.01×10^{-4}		1.56×10^{-4}	
	$B_s \to D_s^{*-} l^+\nu_l$	5.91×10^{-2}		1.46×10^{-2}	

- l indicates an electron or a muon.

The results

			$\langle \mathcal{A}_{FB}^{e} \rangle$	$\langle \mathcal{A}_{FB}^{\mu} \rangle$	$\langle P_L^e \rangle$	$\langle P_L^\mu \rangle$	$\langle P_T^e \rangle (10^{-2})$	$\langle P_T^\mu \rangle$	$\langle C_F^e \rangle$	$\langle C_F^\mu \rangle$	$\langle F_L^e \rangle$	$\langle F_L^\mu \rangle$
$D^+ \to P$	$D^+ \to \eta l^+ \nu_l$	CLFQM	-6.0×10^{-6}	-0.05	1.00	0.84	-0.27	-0.43	-1.50	-1.36	-	-
		CCQM	-6.4×10^{-6}	-0.06	1.00	0.83	-0.28	-0.44	-1.50	-1.32	-	-
		RQM		-0.052	1.00	0.85		-0.40	-1.50	-1.34	-	-
	$D^+ \to \eta' l^+ \nu_l$	CLFQM	-13.2×10^{-6}	-0.10	1.00	0.71	-0.41	-0.57	-1.50	-1.27	-	-
		CCQM	-13.0×10^{-6}	-0.10	1.00	0.70	-0.42	-0.59	-1.50	-1.19	-	-
		RQM		-0.097	1.00	0.72		-0.56	-1.50	-1.20	-	-
	$D^+ \to \pi^0 l^+ \nu_l$	CLFQM	-3.4×10^{-6}	-0.04	1.00	0.90	-0.20	-0.34	-1.50	-1.40	-	-
		CCQM	-4.1×10^{-6}	-0.04	1.00	0.88	-0.22	-0.36	-1.50	-1.37	-	-
		RQM		-0.040	1.00	0.89		-0.36	-1.50	-1.38	-	-
	$D^+ \to \bar{K}^0 l^+ \nu_l$	CLFQM	-5.8×10^{-6}	-0.05	1.00	0.84	-0.27	-0.42	-1.50	-1.36	-	-
		CCQM	-6.4×10^{-6}	-0.06	1.00	0.83	-0.28	-0.43	-1.50	-1.32	-	-
		RQM		-0.053	1.00	0.85		-0.42	-1.50	-1.34	-	-
$D^+ \to V$	$D^+ \to \rho l^+ \nu_l$	CLFQM	-0.24	-0.26	1.00	0.92	-0.10	-0.13	-0.48	-0.40	0.55	0.54
		CCQM	-0.21	-0.24	1.00	0.92	-0.09	-0.13	-0.44	-0.36	0.53	0.51
		RQM	-0.26	-0.28	1.00	0.92		-0.12	-0.42	-0.34	0.52	0.52
	$D^+ \to \omega l^+ \nu_l$	CLFQM	-0.24	-0.26	1.00	0.92	-0.09	-0.12	-0.45	-0.37	0.53	0.53
		CCQM	-0.21	-0.24	1.00	0.92	-0.09	-0.12	-0.43	-0.35	0.52	0.50
		RQM	-0.25	-0.27	1.00	0.93		-0.11	-0.39	-0.32	0.51	0.50
	$D^+ \to \bar{K}^{*0} l^+ \nu_l$	CLFQM	-0.19	-0.22	1.00	0.90	-0.11	-0.15	-0.48	-0.39	0.55	0.54
		CCQM	-0.18	-0.21	1.00	0.91	-0.11	-0.15	-0.47	-0.37	0.54	0.52
		RQM	-0.22	-0.25	1.00	0.90		-0.15	-0.47	-0.37	0.54	0.54
$D_s^+ \to P$	$D_s^+ \to \eta l^+ \nu_l$	CLFQM	-5.6×10^{-6}	-0.05	1.00	0.84	-0.27	-0.43	-1.50	-1.33	-	-
		CCQM	-6.0×10^{-6}	-0.06	1.00	0.84	-0.27	-0.42	-1.50	-1.33	-	-
		RQM		-0.043		0.88		-0.35		-1.37	-	-
	$D_s^+ \to \eta' l^+ \nu_l$	CLFQM	-11.1×10^{-6}	-0.09	1.00	0.74	-0.38	-0.55	-1.50	-1.23	-	-
		CCQM	-11.2×10^{-6}	-0.09	1.00	0.75	-0.38	-0.54	-1.50	-1.23	-	-
		RQM		-0.080		0.77		-0.51		-1.26	-	-
	$D_s^+ \to K^0 l^+ \nu_l$	CLFQM	-5.1×10^{-6}	-0.05	1.00	0.86	-0.25	-0.41	-1.50	-1.35	-	-
		CCQM	-5.0×10^{-6}	-0.05	1.00	0.86	-0.24	-0.39	-1.50	-1.35	-	-
		RQM		-0.038		0.89		-0.34		-1.38	-	-
$D_s^+ \to V$	$D_s^+ \to \phi l^+ \nu_l$	CLFQM	-0.18	-0.21	1.00	0.91	-0.11	-0.14	-0.48	-0.38	0.54	0.53
		CCQM	-0.18	-0.21	1.00	0.91	-0.11	-0.14	-0.43	-0.34	0.53	0.50
		RQM	-0.21	-0.24	1.00	0.90		-0.15	-0.49	-0.35	0.54	0.54
	$D_s^+ \to K^{*0} l^+ \nu_l$	CLFQM	-0.22	-0.25	1.00	0.92	-0.09	-0.12	-0.47	-0.38	0.54	0.54
		CCQM	-0.22	-0.25	1.00	0.92	-0.09	-0.11	-0.40	-0.33	0.51	0.49
		RQM	-0.26	-0.29	1.00	0.92		-0.11	-0.41	-0.33	0.52	0.51

The average values of the observables.

- Theoretical predictions: the covariant confining quark model (CCQM)
  M.A.Ivanov and J.G.Korner, Front.Phys.14,64401(2019)
  and the relativistic quark model(RQM)
  R.Faustov, V.Galkin, and X.-W.Kang Phys.Rev.D 101,013004(2020)
- The lepton mass effect:
  $D_s, B_s \to V$ transition:
  $A_{FB}^{\mu(\tau)}$ are similar to those for $\mathcal{A}_{FB}^{e}$
  $D_s, B_s \to P$ transition:
  $\langle \mathcal{A}_{FB}^{\mu} \rangle / \langle \mathcal{A}_{FB}^{e} \rangle \sim 10^4 \sim m_\mu^2 / m_e^2$
  $\langle \mathcal{A}_{FB}^{\tau} \rangle / \langle \mathcal{A}_{FB}^{e} \rangle \sim 10^7 \sim m_\tau^2 / m_e^2$

The results

- The average values of other observables for the $B_{(s)}$ transitions

		$\langle \mathcal{A}_{FB}^e \rangle$	$\langle \mathcal{A}_{FB}^\tau \rangle$	$\langle P_L^e \rangle$	$\langle P_L^\tau \rangle$	$\langle P_T^e \rangle$	$\langle P_T^\tau \rangle$	$\langle C_F^e \rangle$	$\langle C_F^\tau \rangle$	$\langle F_L^e \rangle$	$\langle F_L^\tau \rangle$
$B^+ \to P$	$B^+ \to \eta l^+ \nu_l$	-0.39×10^{-6}	-0.29	1.00	0.11	-0.64×10^{-3}	-0.86	-1.50	-0.60	-	-
	$B^+ \to \eta' l^+ \nu_l$	-0.49×10^{-6}	-0.31	1.00	0.026	-0.72×10^{-3}	-0.87	-1.50	-0.52	-	-
	$B^+ \to \pi^0 l^+ \nu_l$	-0.35×10^{-6}	-0.28	1.00	0.087	-0.62×10^{-3}	-0.85	-1.50	-0.59	-	-
	$B^+ \to \bar{D}^0 l^+ \nu_l$	-1.04×10^{-6}	-0.36	1.00	-0.32	-1.07×10^{-3}	-0.84	-1.50	-0.27	-	-
$B^+ \to V$	$B^+ \to \rho l^+ \nu_l$	-0.32	-0.39	1.00	0.60	-0.18×10^{-3}	-0.10	-0.39	-0.12	0.51	0.49
	$B^+ \to \omega l^+ \nu_l$	-0.30	-0.36	1.00	0.65	-0.15×10^{-3}	-0.06	-0.42	-0.15	0.51	0.49
	$B^+ \to \bar{D}^{*0} l^+ \nu_l$	-0.22	-0.30	1.00	0.51	-0.29×10^{-3}	-0.10	-0.42	-0.056	0.52	0.45
$B_s \to P$	$B_s \to K^- l^+ \nu_l$	-0.43×10^{-6}	-0.29	1.00	-0.10	-0.72×10^{-3}	-0.86	-1.50	-0.46	-	-
	$B_s \to D_s^- l^+ \nu_l$	-1.05×10^{-6}	-0.36	1.00	-0.33	-1.07×10^{-3}	-0.84	-1.50	-0.26	-	-
$B_s \to V$	$B_s \to K^{*-} l^+ \nu_l$	-0.21	-0.28	1.00	0.65	-0.17×10^{-3}	-0.13	-0.59	-0.26	0.59	0.56
	$B_s \to D_s^{*-} l^+ \nu_l$	-0.22	-0.29	1.00	0.51	-0.29×10^{-3}	-0.10	-0.43	-0.058	0.52	0.45

- $D_{(s)}$, $\langle P_T^\mu \rangle / \langle P_T^e \rangle \sim 10^2 \sim m_\mu / m_e$;
  $B_{(s)}$, $\langle P_T^\tau \rangle / \langle P_T^e \rangle \sim 10^3 \sim m_\tau / m_e$
- $\langle P_L^e \rangle$ equals 1 for all the cases, the term proportional to δ_l almost vanishes;
  In the zero lepton mass limit, $\langle P_T^e \rangle = 0$, $\langle P_L^e \rangle = 1$ for all channels, and $\langle C_F^e \rangle = -1.5$ for the $D_{(s)}/B_{(s)} \to P$ case.

The results

- The ratios of the partial decay rates, $\Gamma_L/\Gamma_T = \langle F_L\rangle/(1-\langle F_L\rangle)$

	CLFQM	CCQM [32]	RQM [37]	Experimental
$D^+ \to \bar{K}^{*0} e^+ \nu_e$	1.21	1.17	1.17	
$D^+ \to \bar{K}^{*0} \mu^+ \nu_\mu$	1.17	1.08	1.17	1.13 ± 0.08 [46]
$D_s \to \phi e^+ \nu_e$	1.17	1.12	1.17	$1.0 \pm 0.3 \pm 0.2$ [52]
$D_s \to \phi \mu^+ \nu_\mu$	1.12	1	1.17	

- Further precise measurement

The results

- Predictions for $F_L^\tau(D_{(s)}^*)$ and $P_L^\tau(D_{(s)}^{(*)})$, compared with other models as well as experimental values. In parenthesis, we also include the value of $F_L^e(D^*)$ for $\bar{B} \to D^* \tau^- \bar{\nu}_\tau$

Observables	Approach	$\bar{B} \to D\tau^-\bar{\nu}_\tau$	$\bar{B} \to D^*\tau^-\bar{\nu}_\tau \, (e^-\bar{\nu}_e)$	$B_s \to D_s\tau^-\bar{\nu}_\tau$	$B_s \to D_s^*\tau^-\bar{\nu}_\tau$
$F_L^\tau(D_{(s)}^*)$	CLFQM	-	0.451 (0.521)	-	0.453
	SM1 [70]	-	0.46 ± 0.04	-	-
	SM2 [71]	-	0.455	-	0.433
	PQCD [72]	-	0.43	-	0.43
	Belle [73]	-	$0.60 \pm 0.08 \pm 0.04$ (0.56 ± 0.02)	-	-
$P_L^\tau(D_{(s)}^{(*)})$	CLFQM	0.32	-0.51	0.33	-0.51
	SM1	0.325 ± 0.09 [74]	-0.497 ± 0.013 [75]	-	-
	SM2 [71]	0.352	-0.501	-	-0.520
	PQCD [72]	0.30	-0.53	0.30	-0.53
	Belle [76]	-	$-0.38 \pm 0.51^{+0.21}_{-0.16}$	-	-

- Discriminate the effects of new operator structure beyond the SM.
- The results $F_L^\tau(D_{(s)}^{(*)})$ agree well within uncertainties.
- The uncertainty for P_L^τ of the Belle measurement is very large.

- The case in which the charge of the lepton is negative $(l^- \bar{\nu}_l)$:

$$\mathcal{A}_{FB}(q^2) = -\frac{3}{4}\frac{\mathcal{H}_P + 4\delta_l \mathcal{H}_{SL}}{\mathcal{H}_{tot}},$$
$$P_L^l(q^2) = -\frac{\mathcal{H}_U + \mathcal{H}_L - \delta_l(\mathcal{H}_U + \mathcal{H}_L + 3\mathcal{H}_S)}{\mathcal{H}_{tot}}, \quad (23)$$
$$P_T^l(q^2) = -\frac{3\pi\sqrt{\delta_l}}{4\sqrt{2}}\frac{\mathcal{H}_P - 2\mathcal{H}_{SL}}{\mathcal{H}_{tot}}.$$

- Forward-backward asymmetry, lepton polarization, and convexity parameters for semileptonic decays of $\bar{B}^0 \to D^+ l^- \bar{\nu}_l$ and $\bar{B}^0 \to D^{*+} l^- \bar{\nu}_l$

		$\langle \mathcal{A}_{FB}^e \rangle$	$\langle \mathcal{A}_{FB}^\tau \rangle$	$\langle P_L^e \rangle$	$\langle P_L^\tau \rangle$	$\langle P_T^e \rangle$	$\langle P_T^\tau \rangle$	$\langle C_F^e \rangle$	$\langle C_F^\tau \rangle$
$\bar{B}^0 \to D^+ l^- \bar{\nu}_l$	CLFQM	-1.04×10^{-6}	-0.36	-1	0.32	1.06×10^{-3}	0.84	-1.5	-0.27
	CCQM	-1.17×10^{-6}	-0.36	-1	0.33		0.84	-1.5	-0.26
$\bar{B}^0 \to D^{*+} l^- \bar{\nu}_l$	CLFQM	0.22	0.054	-1	-0.51	0.46×10^{-3}	0.47	-0.42	-0.056
	CCQM	0.19	0.027	-1	-0.50		0.46	-0.47	-0.062

Theoretical uncertainty

- Attached to form factors: $7\% - 10\%$
- CKM matrix elements: the uncertainty for $|V_{ub}|$ is larger due to the difference between the extractions from the exclusive and inclusive mode, $10\% - 15\%$
- The theoretical uncertainty for the figures about differential distribution $\frac{d\Gamma}{dq^2}$: 10%

Differential decay rate of some channels

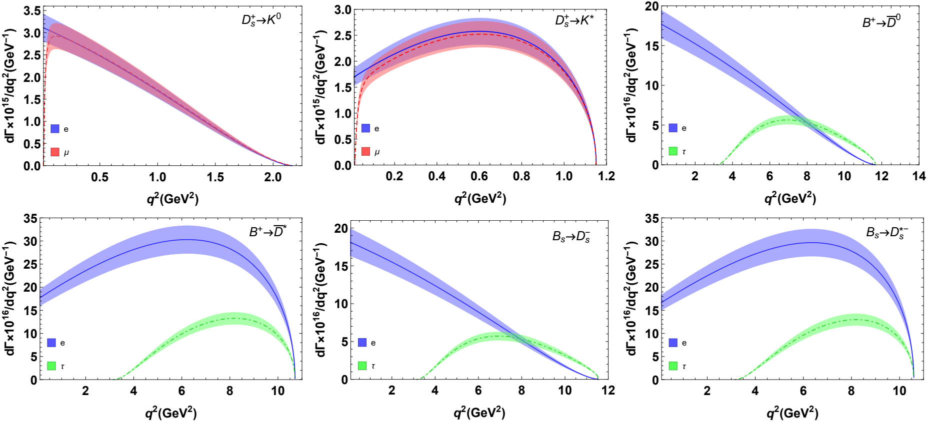

Figure: The solid line denotes the results of the e mode, while the dashed line and dot-dashed line correspond to the μ and τ mode, respectively.

The comparison with experimental data

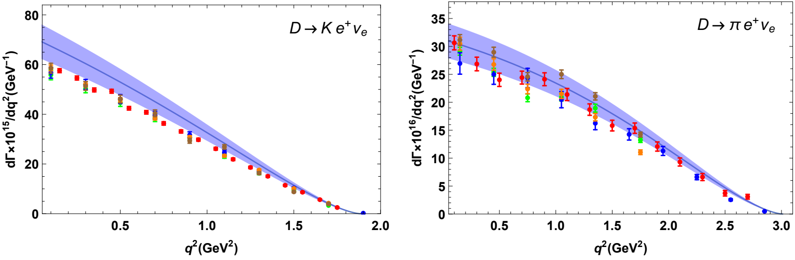

Figure: The experimental data from BESIII for neutral D^0 (red dots with error bars) and charged D^+ (green dots with error bars), BaBar (blue dots and error bars) and CLEO for neutral D^0 (orange dots and error bars) and charged D^+ (brown dots with error bars).

BESIII: M.Ablikim et al.(BESIII), Phys.Rev.D 92,072012(2015); Phys.Rev.D 96,012002(2017)

BaBar: J.Lees et al.(BaBar), Phys.Rev.D 91,052022(2015); B.Aubert et al.(BaBar), Phys.Rev.D 76,052005(2007)

CLEO: D.Besson et al.(CLEO), Phys.Rev.D 80,032005(2009)

The results

- The forward-backward asymmetries

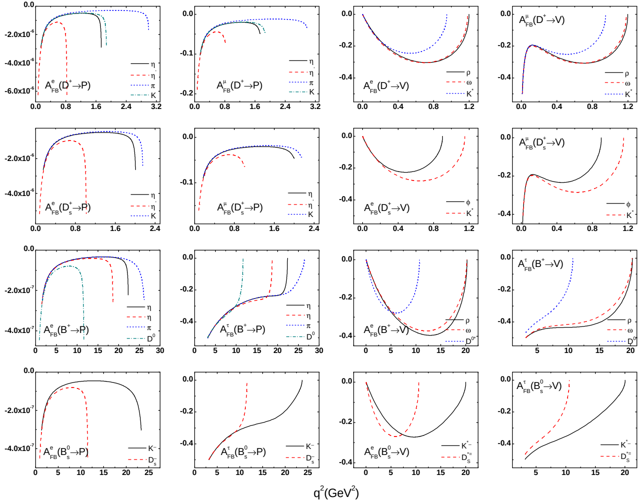

The results

- The longitudinal polarization of a charged lepton

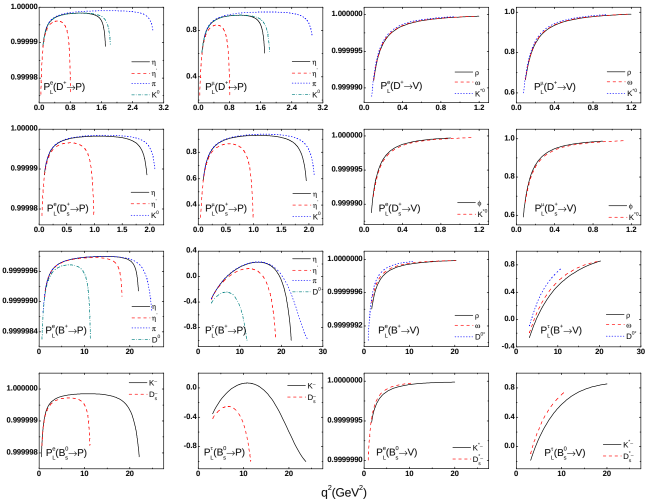

The results

- The transverse polarization of a charged lepton

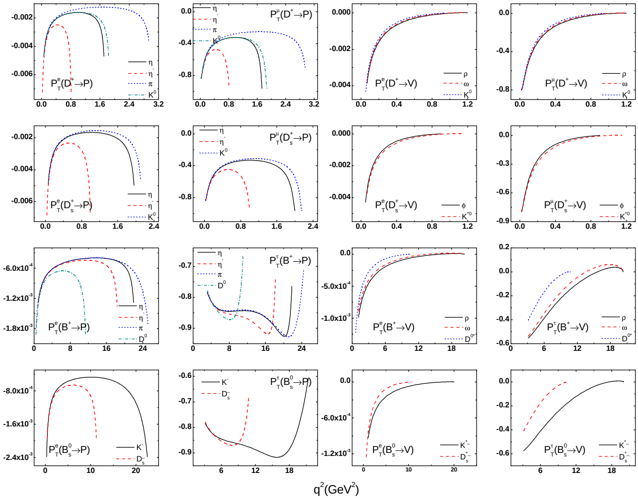

Summary

- helicity amplitudes, helicity component space
- The leptonic and hadronic tensor can be evaluated in two different Lorentz frames.
  $L\left(\lambda_W, \lambda_W'\right)$: in the W rest frame,
  $H\left(\lambda_W, \lambda_W'\right)$: in the D rest frame.
- branching fraction: compared with experimental results for the $D_{(s)}$ decay;
  the predictions for the $B_{(s)}$ decay
- detailed derivation for physical observables
  $F_L^\tau(D^*)$ and $P_L^\tau(D^*)$ for the decay $\bar{B} \to D^* \tau^- \nu_\tau$ from the Belle collaboration
- these polarization observables are crucial inputs for testing and investigating New Physics

THANK YOU